Bending Properties of Ce-TZP/A Nanocomposite Clasps for Removable Partial Dentures

Shinjiro Urano, DDS[a]/Yasuhiro Hotta, DDS, PhD[b]/Takashi Miyazaki, DDS, PhD[c]/Kazuyoshi Baba, DDS, PhD[d]

Purpose: Ceria-stabilized zirconia/alumina nanocomposite (Ce-TZP/A) has excellent fracture toughness and bending strength that could be useful for partial denture framework application. The aim of this study was to investigate the effects of three-dimensional (3D) geometry on the bending and fatigue properties of a model simulation of Ce-TZP/A clasps. **Materials and Methods:** Half oval-shaped Ce-TZP/A rods were prepared in six 3D designs. Specimens were either of standard (width divided by thickness: 2.0/1.0 mm) or flat type (2.5/0.8 mm) cross-sectional areas with taper ratios of 1.0, 0.8, or 0.6. As a comparison, cobalt-chromium (Co-Cr) alloy rods of the same shape as the Ce-TZP/A standard shape rod were prepared. All specimens were subjected to the cantilever test and loaded until fracture. They were also cyclically loaded 10^6 times with various constant displacements, and the maximum displacement prior to fracture was determined for each specimen. Three-dimensional finite element analysis (3D FEA), simulating the cantilever test, was performed to determine the stress distribution during loading. **Results:** Specimens with the standard cross-sectional shape exhibited higher rigidity and higher fracture loads than the flat specimens by the cantilever test. In addition, lower taper ratios were consistently associated with larger displacements at fracture. Fatigue tests revealed that the maximum displacement prior to fracture of Ce-TZP/A specimens was comparable to that of Co-Cr alloy specimens. The 3D FEA showed that specimens with a taper ratio of 0.6 had the least stress concentration. **Conclusions:** Ce-TZP/A clasp specimens with a standard cross-sectional shape and a 0.6 taper ratio exhibited the best bending properties among those tested. *Int J Prosthodont 2015;28:191–197. doi: 10.11607/ijp.4113*

Tooth loss can cause functional and esthetic problems that compromise patients' oral health-related quality of life but can be rectified by prosthodontic treatment. Implant-supported prostheses are gradually replacing conventional prostheses as the treatment of choice; however, removable partial dentures (RPDs) remain a frequently applied treatment intervention because they are less expensive and invasive than implant-retained dentures. Cobalt-chromium (Co-Cr) alloys have long been used as the standard material for RPD frameworks because of their excellent mechanical properties. One of the recognized disadvantages of Co-Cr alloy is its esthetically unacceptable metallic color, requiring complicated fabrication procedures. This material also has the potential to cause a metallic allergy.

To address these problems, modification of the clasp surface and the use of nonmetallic materials as clasps have been tried. Examples include etching the clasp arm and coating it with a layer of tooth-colored acrylic resin,[1–3] using acetal resin clasps available in 16 different colors (Vitapan, VITA Zahnfabrik),[4–6] and using nonmetal clasp dentures that do not include metallic structures.[7,8] All of these alternative approaches have their shortcomings. For instance, coated resin on metal clasps is very likely to crack in the resin layer, and the inherent low elastic modulus of acetal resin clasps requires their considerable enlargement to achieve clinically acceptable retentive forces, which could interfere with the shape of the abutment teeth.

[a]*Postgraduate Student, Showa University School of Dentistry, Department of Prosthodontics, Kita-senzoku, Ohta-ku, Tokyo, Japan.*

[b]*Assistant Professor, Showa University School of Dentistry, Department of Conservative Dentistry, Division of Oral Biomaterials and Technology, Hatanodai, Shinagawa-ku, Tokyo, Japan.*

[c]*Professor, Showa University School of Dentistry, Department of Conservative Dentistry, Division of Oral Biomaterials and Technology, Hatanodai, Shinagawa-ku, Tokyo, Japan.*

[d]*Professor, Showa University School of Dentistry, Department of Prosthodontics, Kita-senzoku, Ohta-ku, Tokyo, Japan.*

Correspondence to: *Prof Kazuyoshi Baba, Department of Prosthodontics, School of Dentistry, Showa University, Kitasenzoku 2-1-1, Oota-ku, Tokyo 145-8515, Japan. Fax: +81 3(3787) 7603. Email: kazuyoshi@dent.showa-u.ac.jp*

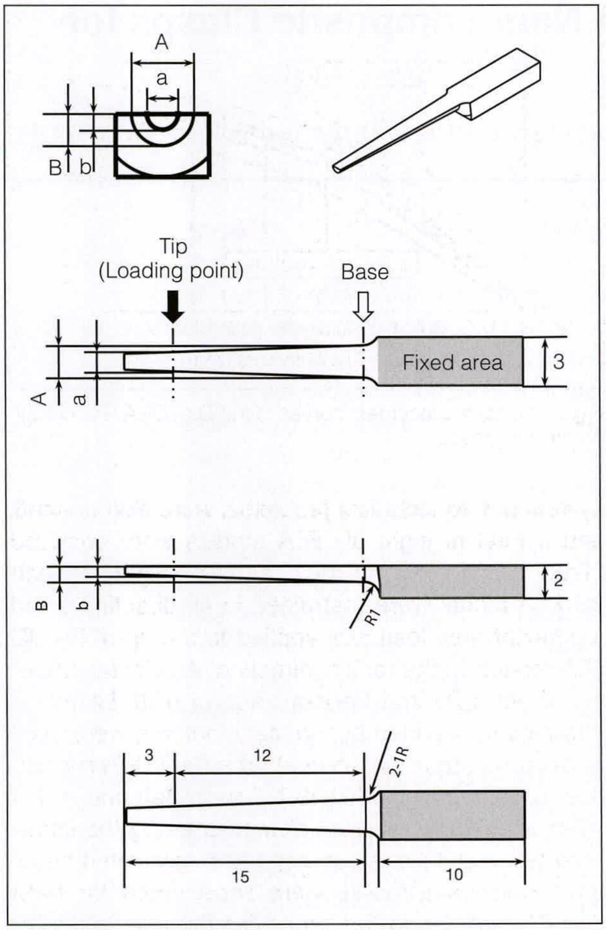

Fig 1 Schematics of the specimens (mm). Tip = loading point; fixed area = portion for fixation to the testing machine; A = width of the base; B = thickness of the base; a = width of the tip; b = thickness of the tip.

Table 1 Cross-Sectional Shape and Taper Ratio of the Specimens (mm)

Group	Taper ratio	Width of base	Thickness of base	Width of tip	Thickness of tip
I	1.0	2.00	1.00	2.00	1.00
	0.8	2.00	1.00	1.60	0.80
	0.6	2.00	1.00	1.20	0.60
II	1.0	2.50	0.80	2.50	0.80
	0.8	2.50	0.80	2.00	0.64
	0.6	2.50	0.80	1.50	0.48

Nonmetal clasp prostheses using thermoplastic resins that do not include a metal structure may distort underocclusal forces and produce excessive stress on the denture ridge.[9,10]

Brittle materials, such as ceramics in general, are not suitable for RPD clasps, which are subjected to repetitive bending during denture insertion and removal, and, therefore, need to be flexible. Ceria-stabilized zirconia/alumina nanocomposite (Ce-TZP/A; P-nanoZR, Panasonic Healthcare),[11] which is composed of a matrix of 10 mol% CeO_2-stabilized TZP containing 30 vol% Al_2O_3 as a second phase, is a newer generation of zirconia that can be processed by dental computer-aided design/computer-assisted manufacture (CAD/CAM) systems. Because of its higher bending strength and fracture toughness compared to conventional yttrium partially stabilized zirconia (Y-TZP),[11] Ce-TZP/A has been used for the frames of all-ceramic fixed prostheses. Ce-TZP/A also exhibits a similar elastic modulus to that of Co-Cr alloys and better bending properties than Y-TZP, indicating that this material may be suitable for use in RPD frameworks. Such frameworks would have a significant impact on clinical dentistry because they can solve the three forementioned disadvantages of Co-Cr alloy frameworks. Specifically, Ce-TZP/A clasps may be esthetically superior, applicable to patients with metal allergies, and compatible with processing using a dental CAD/CAM system.

For clasps to function over the long term without permanent deformation or fracture, their elastic limit must be sufficiently higher than the amplitude of clasp strain during RPD insertion and removal, and the fatigue characteristics after repetitive bending, even if they are below the elastic limit, must remain stable. The aim of this study was to investigate the effect of the three-dimensional (3D) geometry of a Ce-TZP/A model and simulated clasps on their bending and fatigue characteristics.

Materials and Methods

Specimen Preparation

Half-oval-shaped Ce-TZP/A rods of 15 mm length were prepared by a CAD/CAM system. The loading point was located 12 mm from the specimen holder to simulate the circumferential clasp for the molar (Fig 1). Six different specimen types were placed in one of two groups: group I, standard (width/thickness: 2.0/1.0 mm) or group II, flat type (2.5/0.8 mm) cross-sectional areas with taper ratios of 1.0, 0.8, or 0.6 (ratio of cross-sectional dimension at the loading point to the base point) (Fig 1, Table 1). The group I standard cross-sectional shapes were the same as the standard Co-Cr alloy clasps used for molars.[12,13] In addition, specimens with a taper ratio of 0.4 were processed by a dental CAD/CAM system. However, fracture occurred frequently during processing, and, therefore, these specimens were not tested in this study. As a comparison, Co-Cr alloy specimens in the same shape as the Ce-TZP/A group I were prepared. Wax patterns for casting were first manufactured

Table 2 Cross-Sectional Shape and Taper Ratio Simulated by the 3D FEA (mm)

Group	Taper ratio	Width of base	Thickness of base	Width of tip	Thickness of tip
I	1.0	2.00	1.00	2.00	1.00
	0.8	2.00	1.00	1.60	0.80
	0.6	2.00	1.00	1.20	0.60
	0.4	2.00	1.00	0.80	0.40
II	1.0	2.50	0.80	2.50	0.80
	0.8	2.50	0.80	2.00	0.64
	0.6	2.50	0.80	1.50	0.48
	0.4	2.50	0.80	1.00	0.32

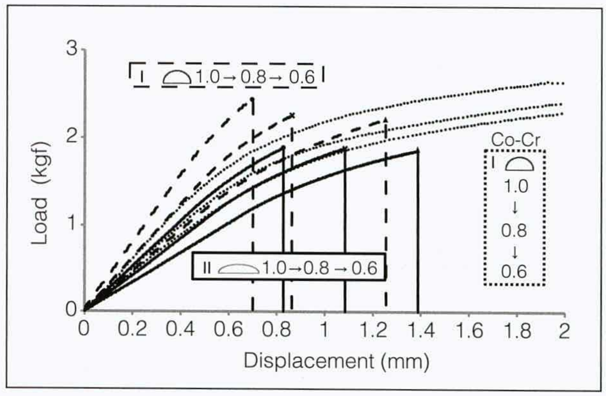

Fig 2 Load-displacement curves of the Ce-TZP/A and cobalt-chromium groups.

with a 3D printer (DDLS-SP-1, DICO) using 3D digital data from the Ce-TZP/A group I specimens. These patterns were embedded, and then the Co-Cr alloy (Heraenium, Heraeus Kulze) were casted following the manufacturer's instructions.

Cantilever Test

The specimens were placed in a universal testing machine (Instron 1125-5500R, Instron) and loaded until fracture by applying radial direction force at the tip of each clasp arm at a crosshead speed of 0.5 mm per minute. The load-displacement curves were recorded and the effects of the cross-sectional design and taper ratios on the loads and the displacements at Ce-TZP/A fracture were evaluated using two-way analysis of variance followed by Tukey tests ($P < .01$). In addition, the maximum principal stress at fracture was calculated using the load and displacement data of the Ce-TZP/A specimens with a taper ratio of 1.0.

Fatigue Test

Each specimen was placed in a testing machine (Servopulsar, Shimadzu) and repeatedly loaded for 10^6 cycles[14] under constant deflection by application of a radial direction force at the tip of each specimen at a frequency of 5 Hz. The maximum displacement amplitude of each specimen that did not cause fracture was determined.

Finite Element Analysis

A 3D finite element analysis (3D FEA) was performed by modeling the same conditions as the cantilever test. The 3D FEA models, which were created with 3D FEA software (ANSYS V10.0 FEM, ANSYS), were theoretically identical to the specimens used for the cantilever test. Models with the taper ratio of 0.4 for both groups, which could not be processed by the CAM system due to technical problems, were also created, and a total of eight 3D FEA models were analyzed (Table 2). All nodes at the fixed area (Fig 1) of each 3D FEA model were restrained in all directions, and a concentrated load was applied to the tip of the 3D FEA models in the radical direction. An elastic modulus of 245 GPa and Poisson ratio of 0.30, based on information provided by the manufacturer, were used in the program to approximate the Ce-TZP/A properties. The model included 18,785 to 22,390 nodes and 4,706 to 6,775 tetrahedral elements. Using the cantilever test results, contour maps with calculated maximum principal stresses were constructed for each 3D FEA model, and the stress distributions in the 3D FEA models with different cross-sectional shapes and taper ratios were visually analyzed. Furthermore, the magnitudes of the maximum principal stresses were calculated for the condition where a load of 0.5 kgf was applied to the tip of the 3D FEA models.

Results

Cantilever Test

Fracture of the Ce-TZP/A specimens consistently occurred at the base region of each specimen independent of the 3D geometry. The maximum principal stress at fracture, estimated from the data obtained from the Ce-TZP/A specimens with taper ratio 1.0, was approximately 1,100 MPa (group I: 1,083 ± 41 MPa, group II: 1,161 ± 85 MPa).

Figure 2 displays the load-displacement curves for the Ce-TZP/A groups I and II and the Co-Cr alloy group. The rigidity of Ce-TZP/A group I as evaluated by the slope of the curve was higher than that of Ce-TZP/A group II when the taper ratio was controlled, and rigidity declined with decreasing taper ratio for each group. The rigidity of Ce-TZP/A group I was comparable to or slightly higher than that of Co-Cr alloy for each taper ratio.

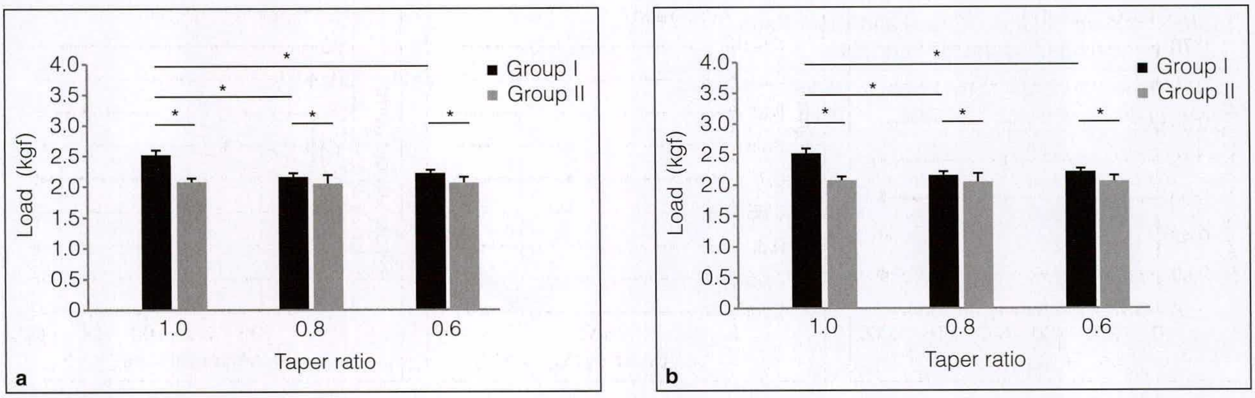

Fig 3 **(a)** Loads at fracture. **(b)** Displacements at fracture. *$P < .01$.

Table 3 Loads and Displacements (Means ± SDs) at Fracture for the Six Specimen Types (n = 5)

Group	Taper ratio	Load (kgf)	Displacement (mm)
I	1.0	2.52 ± 0.06	0.69 ± 0.06
	0.8	2.16 ± 0.06	0.86 ± 0.03
	0.6	2.22 ± 0.05	1.23 ± 0.06
II	1.0	1.88 ± 0.06	0.81 ± 0.03
	0.8	1.85 ± 0.12	1.04 ± 0.06
	0.6	1.86 ± 0.08	1.39 ± 0.03

Table 4 Results of Two-Way Analysis of Variance Determining the Effects of the Cross-Sectional Area Design and the Taper Ratio on the Loads and Displacements

	df	Sum of squares	F	*P*
Load				
Cross-sectional shape	1	1.43	230	< .0001
Taper ratio	2	0.21	17.0	< .0001
Cross-sectional shape × taper ratio	2	0.17	13.7	.0001
Displacement				
Cross-sectional shape	1	0.17	74.9	< .0001
Taper ratio	2	1.62	358	< .0001
Cross-sectional shape × taper ratio	2	0.01	1.13	.3384

Table 5 Maximum Displacements Applied During the Fatigue Test that Did Not Cause Fracture for the Ce-TZP/A and Cobalt-Chromium (Co-Cr) Groups

		Displacement (mm)	
Group	Taper ratio	Ce-TZP/A	Co-Cr
I	1.0	0.50	0.50
	0.8	0.70	0.70
	0.6	0.85	0.90
II	1.0	0.65	
	0.8	0.80	
	0.6	0.90	

Tables 3 and 4 and Fig 3 summarize the amplitudes of the loads and displacement of Ce-TZP/A specimens at fracture and the effects of the cross-sectional shape and the taper ratio. The most significant finding was that group I exhibited consistently and significantly higher loads at fracture than group II. Another significant finding was that lower taper ratios were associated with larger displacements at fracture ($P < .01$).

Fatigue Test

Table 5 shows the maximum displacements applied during the fatigue test that did not cause fracture for Ce-TZP/A groups I (Fig 4) and II and the Co-Cr alloy group. The maximum displacements of Ce-TZP/A group I were comparable to those of the Co-Cr alloy group and were lower than those of Ce-TZP/A group II for each taper ratio. In each group, lower taper ratios were associated with larger displacements. Overall, the maximum displacement prior to fracture was larger than 0.5 mm in all specimens.

Finite Element Analysis

Figure 5 shows the contour maps of Ce-TZP/A group I and II models with a maximum principal stress of 1,000 MPa, which was assumed to be the load just prior to fracture because the maximum principal stress at fracture was approximately 1,100 MPa, estimated using the results of the cantilever test. The maximum principal stress was consistently observed at the base of each model except for the model with taper ratio 0.4, where fracture did actually occur in the specimens assessed by the cantilever test. In both groups, a smaller taper ratio was associated with less stress concentration. However, specimens with taper ratio 0.4 showed concentration of high stress at the middle site. Overall, specimens with taper ratio 0.6 showed the least concentration of stress.

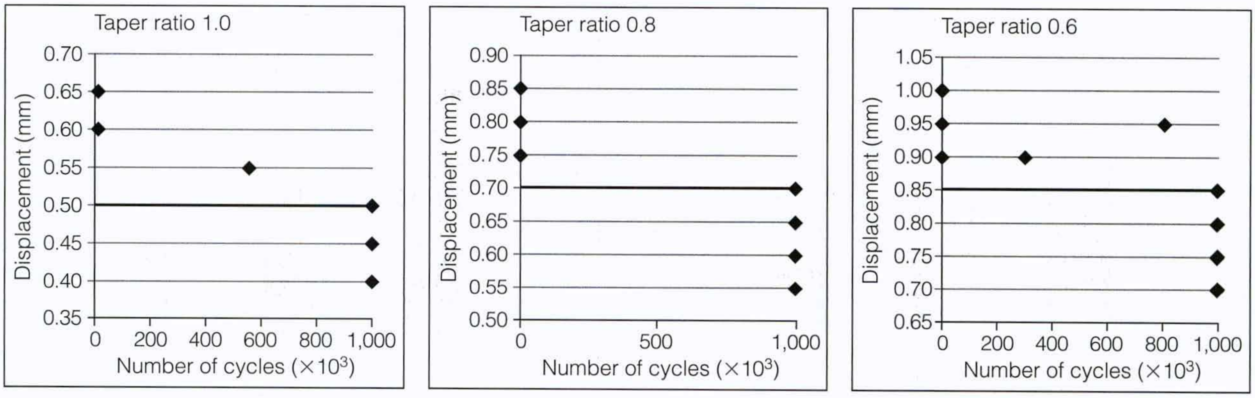

Fig 4 Effect of the taper ratio on the fatigue property of the Ce-TZP/A group I specimens. The displacements prior to fracture are plotted as a function of the cycle number. The maximum displacement, which did not cause fracture after 10^6 cyclic loadings, was 0.5 mm for the specimens with 1.0 taper ratio *(left)*, 0.7 mm for those with 0.8 taper ratio *(center)*, and 0.85 mm for those with 0.6 taper ratio *(right)*.

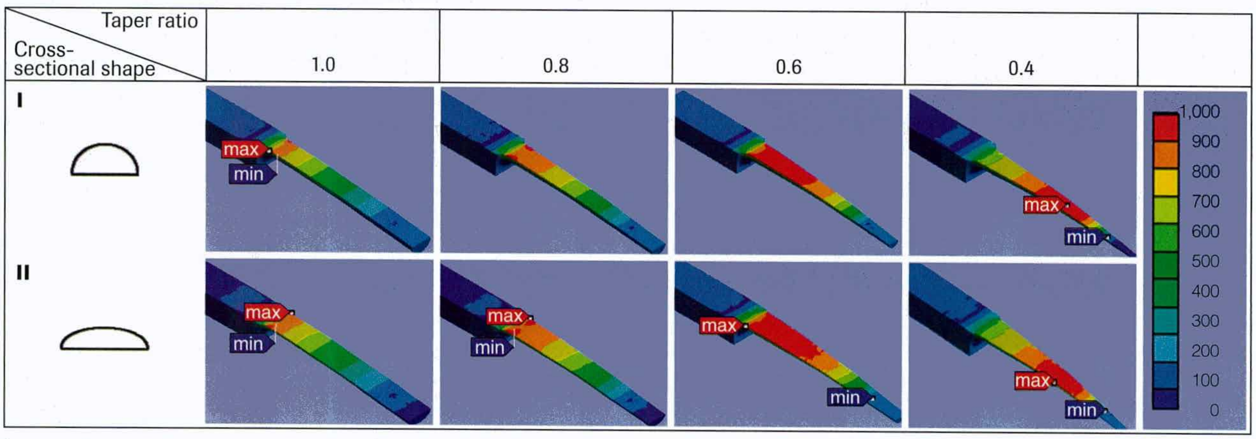

Fig 5 Contour maps showing a maximum principal stress value of 1,000 MPa.

Figure 6 displays the maximum principal stress values when a load of 0.5 kgf was applied to the tip of each 3D FEA model. The maximum principal stress of Ce-TZP/A group I was lower than that of Ce-TZP/A group II for each taper ratio. The maximum principal stress value decreased with decreasing taper ratios, except for a ratio of 0.4, where it increased.

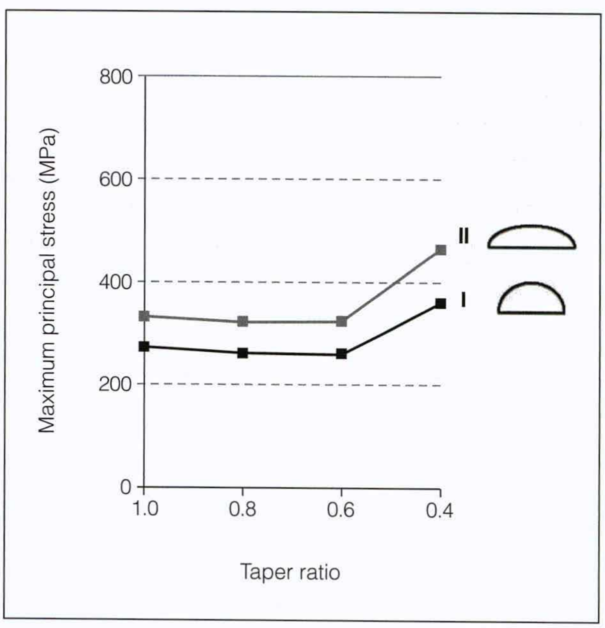

Fig 6 Maximum principal stress when a load of 0.5 kgf was applied to the tip of the 3D FEA models.

Discussion

Bates[15] and Ney[16] reported that the ideal clasp arm should have a half-round cross-sectional shape and be uniformly tapered from its point of attachment at the clasp body to its tip in order to achieve flexibility. Such half-round and tapered designs have been the standard for Co-Cr alloy clasps used in the clinical setting, and the group I design was created based on them. In addition, because thinner and wider clasp arm designs were recommended for reducing fatigue and/or permanent deformation,[17,18] the authors also investigated flat type specimens (group II) for comparison.

For long-term use of RPD clasps, the displacement of the clasp tip that occurs during insertion and removal of the denture must be within the elastic limit.[15,19] The standard design for Co-Cr alloy clasps suggested in the literature was used in this study because the elastic modulus of Ce-TZP/A is comparable to that of Co-Cr alloy. The authors' finding that the maximum displacements prior to fracture were more than 0.5 mm in all designs tested suggested that the risk of fracture for Ce-TZP/A clasps is, in theory, low if the clasp is designed to use the same amount of undercut (0.25 mm)[20] as used for Co-Cr alloy clasps.

It should be noted, however, that the Ce-TZP/A specimens fractured during the cantilever test, whereas the Co-Cr specimens did not. This difference was expected because of the inherent brittle characteristics of ceramics despite the higher fracture strength of Ce-TZP/A compared to Y-TZP. Therefore, this study aimed to find a 3D clasp design that is less susceptible to fracture. The results indicated that the cross-sectional area had a significant effect on the load at fracture. Group I (standard design) exhibited a much higher fracture load than group II (flat design). For clinical applications, clasp arms need to exert an appropriate retentive force. Ideally, the fracture load should be much greater than this force in order to avoid clasp fractures. In this regard, the standard cross-sectional design might have the advantage over the flat cross-sectional design. In addition to higher fracture loads, the clasps with the standard design need a smaller undercut than the flat design to exert a given retentive force because of their higher rigidity, which is also advantageous for brittle materials such as zirconia. Furthermore, the results of the FEA analysis showed that the maximum principal stress of group I was lower than that of group II when a constant load was applied (Fig 6).

Although the fatigue test indicated that group II exhibited slightly higher fatigue resistance than the standard design, both Ce-TZP/A groups exhibited excellent fatigue resistance, comparable to that of Co-Cr alloy (Table 5). The maximum displacement values prior to fracture were higher than 0.5 mm in all of the specimens, which is twice as large as the magnitude of the undercut that Co-Cr alloy clasps need to exert for appropriate retention. Therefore, fatigue destruction of Ce-TZP/A clasps is unlikely to happen or is as likely as for Co-Cr alloy clasps.

Specimens with taper ratio of 0.6 showed the largest displacement at comparable loads when compared with specimens with the other two taper ratios, suggesting that this taper ratio is the most appropriate among the three designs. This was also supported by the FEA analysis, which showed that the 3D FEA models with 0.6 taper had the least stress concentration in the model (Fig 5).

In this study, the authors examined only straight type specimens, which are different from the clasp design used clinically, and the curvature of the clasp could affect its rigidity and stress distribution.[15,18,21,22] Furthermore, previous studies have indicated that the retentive force of the clasp is affected by the contour and curvature radius of the abutment tooth as well as the friction coefficient between the abutment tooth and the clasp.[23–25] In future studies, these factors should also be examined to determine the optimal Ce-TZP/A clasp design.

This laboratory report indicated that the selected and tested specimens with 2.0-mm width, 1.0-mm thickness at the base, and 0.6 taper ratio exhibit the best bending properties with acceptable fatigue properties for the different studied designs. These preliminary data established a basic comparison set for applying Ce-TZP/A as a clasp material and suggests promise for additional study, especially in a clinical context.

Conclusions

Using Ce-TZP/A specimens, mechanical testing, and 3D FEA, the authors elucidated the effects of 3D design geometries on the bending and fatigue properties of model and simulated zirconia clasps. The results showed that specimens with 2.0-mm width, 1.0-mm thickness, and 0.6 taper ratio demonstrated the best bending properties with acceptable fatigue properties.

Acknowledgments

The authors are grateful to Panasonic Health Care, Ehime, Japan, for manufacturing the Ce-TZP/A specimens and to Drs Azusa Mabuchi, Keita Tachi, Hirotaka Nishiyama, Shinpei Tanaka, Hiroaki Tsukasaki, and Mari Kobayashi, Showa University School of Dentistry, for their technical support on preparation of the experiments, FEA analyses, and statistical analyses. The authors reported no conflicts of interest related to this study.

References

1. de Delgado MM, Garcia LT, Rudd KD. Camouflaging partial denture clasps. J Prosthet Dent 1986;55:656–660.
2. Snyder HA, Duncanson MG, Johnson DL, Bloom J. Effects of clasp flexure on a 4-META adhered light-polymerized composite resin. Int J Prosthodont 1991;4:364–370.
3. Ozcan M. The use of chairside silica coating for different dental applications: A clinical report. J Prosthet Dent 2002;87:469–472.
4. Fitton JS, Davies EH, Howlett JA, Pearson GJ. The physical properties of a polyacetal denture resin. Clin Mater 1994;17: 125–129.
5. Turner JW, Radford DR, Sherriff M. Flexural properties and surface finishing of acetal resin denture clasps. J Prosthodont 1999;8:188–195.

6. Arda T, Arikan A. An in vitro comparison of retentive force and deformation of acetal resin and cobalt-chromium clasps. J Prosthet Dent 2005;94:267–274.
7. Goiato MC, Panzarini SR, Tomiko C, Luvizuto ER. Temporary flexible immediately removable partial denture: A case report. Dent Today 2008;27:114–116.
8. Kaplan P. Flexible removable partial dentures: Design and clasp concepts. Dent Today 2008;27:120–122.
9. Fueki K, Ohkubo C, Yatabe M, et al. Clinical application of removable partial dentures using thermoplastic resin—Part I: Definition and indication of non-metal clasp dentures. J Prosthodont Res 2014;58:3–10.
10. Jiao T, Chang T, Caputo AA. Load transfer characteristics of unilateral distal extension removable partial dentures with polyacetal resin supporting components. Aust Dent J 2009; 54:31–37.
11. Nawa M, Nakamoto S, Sekino T, Niihara K. Tough and strong Ce-TZP/Alumina nanocomposites doped with titania. Ceram Int 1998;24:497–506.
12. Jelenko JF. Partial Dentures: Surveying, Designing, Construction. New York: J.F. Jelenko & Co; 1966:22–26.
13. Carr AB, Brown DT. McCracken's Removable Partial Prosthodontics, 12th ed. St Louis: Elsevier Mosby; 1981:88–92.
14. Wiskott HW, Nicholls JI, Belser UC. Stress fatigue: Basic principles and prosthodontic implications. Int J Prosthodont 1995;8:105–116.
15. Bates JF. The mechanical properties of the cobalt-chromium alloys and their relation to partial denture design. Br Dent J 1965;119:389–396.
16. Ney JM. Planned Partials. Hartford, CT: The J.M. Ney, 1963: 84–88.
17. Morris HF, Asgar K, Brudvik JS, Winkler S, Roberts EP. Stress-relaxation testing. Part IV: Clasp pattern dimensions and their influence on clasp behavior. J Prosthet Dent 1983;50:319–326.
18. Sato Y, Yuasa Y, Akagawa Y, Ohkawa S. An investigation of preferable taper and thickness ratios for cast circumferential clasp arms using finite element analysis. Int J Prosthodont 1995; 8:392–397.
19. Cheng H, Xu M, Zhang H, Wu W, Zheng M, Li X. Cyclic fatigue properties of cobalt-chromium alloy clasps for partial removable dental prostheses. J Prosthet Dent 2010;104:389–396.
20. Bates JF. Removable Partial Denture Construction. 2nd ed. Bristol: John Wright and Sons, 1978:29.
21. Johnson DL, Stratton RJ, Duncanson MG. The effect of single plane curvature on half-round cast clasps. J Dent Res 1983; 62:833–836.
22. Sato Y, Tsuga K, Abe Y, Akagawa Y. Finite element analysis of the effect of vertical curvature on half-oval cast clasps. J Oral Rehabil 1999;26:554–558.
23. Warr JA. Friction and partial denture retention. J Dent Res 1959;38:1066–1074.
24. Yuasa Y, Sato Y, Ohkawa S, Nagasawa T, Tsuru H. Finite element analysis of the relationship between clasp dimensions and flexibility. J Dent Res 1990;69:1664–1668.
25. Sato Y, Abe Y, Yuasa Y, Akagawa Y. Effect of friction coefficient on Akers clasp retention. J Prosthet Dent 1997;78:22–27.

Literature Abstract

Flapless versus conventional flapped dental implant surgery: A meta-analysis

This study analyzed implant failure rates, postoperative infection, and marginal bone loss in patients with dental implants inserted by a flapless surgical technique versus the open flap technique. An electronic search undertaken in March 2014 yielded 23 eligible publications for analysis, all of which included human studies. The estimates of relative effect for dichotomous outcomes were expressed in risk ratio (RR) and in mean difference (MD) in millimeters, with a 95% confidence interval (CI). From these studies, a total of 1,648 implants were placed through flapless surgery, with 51 failures (3.09%), and 1,848 implants were placed through open flap surgery, with 32 failures (1.73%). The test for overall effect showed that the two techniques statistically affected implant failure rates with a RR of 1.75 (95% CI: 1.07 to 2.86) for the use of flapless surgery. However, sensitivity analysis showed when studies with high risk and low risk bias were pooled separately, no significant effects of flapless surgery on the occurrence of postoperative infection (P = .96; RR: 0.96, 95% CI: 0.23 to 4.03) or on marginal bone loss (P + .16; MD: –0.07 mm, 95% CI: –0.16 to 0.03) were found. The authors concluded that though the different surgical techniques statistically affected implant failure, the results have to be interpreted with caution due to the limitations of this study. The lack of control of confounding factors, the presence of inherently flawed retrospective studies and the lack of data led them to believe that future double-blinded randomized controlled trials with larger patient samples will help determine the true outcome of flapless implant surgery on patient outcome variables.

Chrcanovic BR, Albrektsson T, Wennerberg A. *PLoS One* 2014; 20;9(6):e100624. **doi:** 10.1371/journal.pone.0100624. eCollection 2014. **References:** 43. **Reprints:** Bruno Ramos Chrcanovic, Department of Prosthodontics, Faculty of Odontology, Malmö University, Carl Gustafs väg 34, SE-205 06, Malmö, Sweden. Fax: +46 40 6658503. Email: bruno.chrcanovic@mah.se—*Teo Juin Wei, Singapore*